Catal Lett (2008) 121:70–76
DOI 10.1007/s10562-007-9294-3

An Investigation of Catalytic Activity for CO Oxidation of $CuO/Ce_xZr_{1-x}O_2$ Catalysts

Shu-Ping Wang · Tong-Ying Zhang · Yan Su · Shu-Rong Wang · Shou-Min Zhang · Bao-Lin Zhu · Shi-Hua Wu

Received: 1 July 2007 / Accepted: 30 September 2007 / Published online: 11 October 2007

Abstract A series of $CuO/Ce_xZr_{1-x}O_2$ catalyst powders with different Ce/Zr ratio were prepared via an impregnation method and characterized by X-ray diffraction (XRD), Fourier transform Raman (FT-Raman), H_2-Temperature-programmed reduction (TPR) and X-ray photoelectron spectra techniques. The catalytic properties of the catalysts were evaluated by means of a microreactor-GC system. XRD results showed that the addition of CuO had no effect on the crystalline lattice of the support. The structures of the $Ce_xZr_{1-x}O_2$ samples were confirmed by XRD analyses and FT-Raman results. The H_2-TPR profiles for these catalysts had three peaks, which could be attributed to the reduction of three kinds of CuO species, i.e., the highly dispersed CuO, the larger CuO species and the bulk CuO. The TPR analyses and catalytic property tests indicated that the Ce/Zr ratio of $CuO/Ce_xZr_{1-x}O_2$ had an effect on the dispersion degree of CuO and the catalytic activity of the catalysts.

Keywords CO oxidation · $Ce_xZr_{1-x}O_2$ · $CuO/Ce_xZr_{1-x}O_2$ · Catalytic activity

1 Introduction

In recent years, the protection of the environment is receiving much more attentions than ever before. Carbon monoxide, produced during the combustion of fuels in factories and automotive engines, has been considered as a major air pollution. Several catalysts have been investigated for the CO catalytic oxidation at low-temperature [1].

Copper oxide and supported copper oxides have been extensively investigated during the past decades. Most of the studies have focused on the supported copper oxides, such as CuO/ZnO [2], CuO/ZrO_2 [3], CuO/ThO_2 [4], CuO/TiO_2 [5], CuO/Fe_2O_3 [6] and CuO/Al_2O_3 [7]. Recently, there is much interest in CuO/CeO_2 catalysts due to the high activity induced by the interaction of the surface copper species with CeO_2 [8, 9]. The major role of cerium oxide in the catalysts is to control the oxygen concentration by storage and release under the reaction environment [10]. However, as a support, ceria will result in significant efficiency decrease of the catalysts under thermally harsh environment. Therefore, many studies have focused on Ce–Zr mixed oxide [11–14]. In the mixed oxide of $Ce_xZr_{1-x}O_2$, Zr^{4+} ion partially substitutes for Ce^{4+} in the lattice of CeO_2, forming a solid solution. Compared to pure ceria, the Ce–Zr mixed oxides can maintain the reversible Ce^{3+}/Ce^{4+} redox property even after exposure to the reduction condition above 1,173 K [12] and show the improved thermal resistance and better catalytic activity at higher temperature [13, 14]. Thus, copper oxides supported on $Ce_xZr_{1-x}O_2$ catalysts are of the greatest interest to enhance CO oxidation recently.

So far, many methods have been used to prepare the cerium–zirconium mixed oxides, such as, co-precipitation [15], high energy ball milling [16], sol–gel [17] and hydrothermal synthesis [18]. Among these methods, hydrothermal synthesis always has the main advantages in preparing highly crystallized nano-materials with controlled shape, size and orientation and has been employed to prepare various materials. In previous work, we had prepared the samples by co-precipitation and citrate

S.-P. Wang · T.-Y. Zhang · Y. Su · S.-R. Wang · S.-M. Zhang · B.-L. Zhu · S.-H. Wu (✉)
Department of Chemistry, Nankai University, Tianjin 300071, China
e-mail: wushh@nankai.edu.cn

method, and the catalytic activities of the catalysts for CO oxidation were also investigated [13, 19]. However, the catalytic activities were not very satisfactory. In this paper, to improve the catalytic property of the catalysts, the mixed oxide $Ce_xZr_{1-x}O_2$ was synthesized by a hydrothermal route and used as support for a series of $CuO/Ce_xZr_{1-x}O_2$ catalysts. The catalysts were characterized by X-ray diffraction (XRD), Fourier transform Raman (FT-Raman), H_2-Temperature-programmed reduction (TPR) and X-ray photoelectron spectra (XPS) techniques and their catalytic activities were evaluated by using a microreactor-GC system. The influence of Ce/Zr molar ratio on the structure and catalytic behaviors of $CuO/Ce_xZr_{1-x}O_2$ catalysts was investigated.

2 Experimental

2.1 Preparation of Supports and Catalysts

The supports $Ce_xZr_{1-x}O_2$ with x = 1, 0.8, 0.6, 0.5, 0.4, 0.2 and 0 were prepared via a hydrothermal route by using $Ce(NO_3)_3{\cdot}6H_2O$ and $Zr(NO_3)_4{\cdot}5H_2O$ as precursors. Appropriate amounts of $Ce(NO_3)_3{\cdot}6H_2O$ and $Zr(NO_3)_4{\cdot}5H_2O$ were dissolved into 80 ml distilled water in a 100 ml Teflon bottle. 0.96 g urea $[CO(NH_2)_2]$ was slowly added into above solution under vigorous stirring in order to keep the local concentration homogeneous. After stirring for about one hour, the Teflon bottle was put into a stainless steel vessel and the vessel was sealed tightly. Then it was placed in an oven and subjected to hydrothermal treatment at 160 °C for 24 h. After hydrothermal treatment, white precipitates were formed. The precipitates were washed several times with de-ionized water, dried at 80 °C overnight in the oven and then calcined at 500 °C in a muffle furnace for 4 h. The resulting yellow powders were obtained.

$CuO/Ce_xZr_{1-x}O_2$ were prepared by the impregnation method using an aqueous solution of $Cu(NO_3)_2{\cdot}3H_2O$ and the prepared $Ce_xZr_{1-x}O_2$ support. The prepared samples were dried at 80 °C overnight and calcined in a muffle furnace at 500 °C for 4 h. The catalysts were obtained and the CuO loading was 5 wt.%.

2.2 Catalyst Characterization

X-ray diffraction patterns were obtained by using a DMAX-2500 diffractometer (Rigaku Corporation) with Cu Kα radiation in the scanning region of 2θ = 10–80°. The working voltage and current of the X-ray tube were 40 kV and 100 mA. The average crystalline size was calculated from the peak width according to Scherrer's equation.

Fourier transform Raman spectra were recorded with a RTS 100/S FT-RAMAN spectrometer (BRUKER, Germany) with liquid N_2 detector, using the 1,064 nm excitation line of Nd-YAG laser. The dates were collected by keeping the power at 70 mW. The sample powders were pressed into small disc and then mounted on the analytic chamber.

Temperature-programmed reduction experiments were performed on a TPDRO 1100 apparatus supplied by Thermo-Finnigan Company. 50 mg of the sample was heated from room temperature to 1,000°C at a rate of 10°C/min under a mixture of 5% H_2 in N_2 flowing (20 mL min^{-1}). The H_2 uptake amount during the reduction was measured by a gas chromatorgraph equipped with a thermal conductivity detector (TCD).

X-ray photoelectron spectra were analyzed on a PHI-1600 spectrometer (U.S.A) using Mg Kα radiation for exciting photoelectrons. X-ray source was operated at an accelerating voltage of 15 kV and 250 W. The pressure in the ion-pumped analysis chamber was maintained at 1.1 Pa $\times$ 10^{-7} Pa during data acquisition. All binding energies (BE) were referenced to the adventitious C 1s line at 284.6 eV.

2.3 Catalytic Activity Test

The catalytic activity measurements of the catalysts for CO oxidation were carried out in a fixed bed flow microreactor (7 mm i.d.) under atmospheric pressure. 0.05 g of prepared catalyst powders were diluted with 2.00 g SiO_2 (≥90 mesh) uniformly. The airflow rate was 33.3 mL/min and the CO gas flow rate was 0.5 mL/min. The reactant and product compositions were analyzed on-line by a GC-508A equipped with TCD.

3 Results and Discussion

The XRD patterns of the prepared cerium–zirconium mixed oxides and the $CuO/Ce_xZr_{1-x}O_2$ catalysts are shown in Fig. 1. The $CuO/Ce_xZr_{1-x}O_2$ catalysts had the same patterns as the pure $Ce_xZr_{1-x}O_2$ supports for every x-value, which indicated that the addition of CuO had no effect on the crystalline lattice of the support. The XRD patterns of CeO_2 and $Ce_{0.8}Zr_{0.2}O_2$ can be assigned to a typical cubic fluorite structure. No extra peaks associated with ZrO_2 were observed for the $Ce_{0.8}Zr_{0.2}O_2$ sample, which implied that ZrO_2 was incorporated into the CeO_2 lattice to form a solid solution while maintaining the fluorite structure. As the fraction of Zr (1–x) exceeded 0.2, the peaks assigned to tetragonal ZrO_2 (t-ZrO_2) appeared. The $Ce_xZr_{1-x}O_2$ samples with x = 0.6, 0.5 and 0.4 showed a small degree of

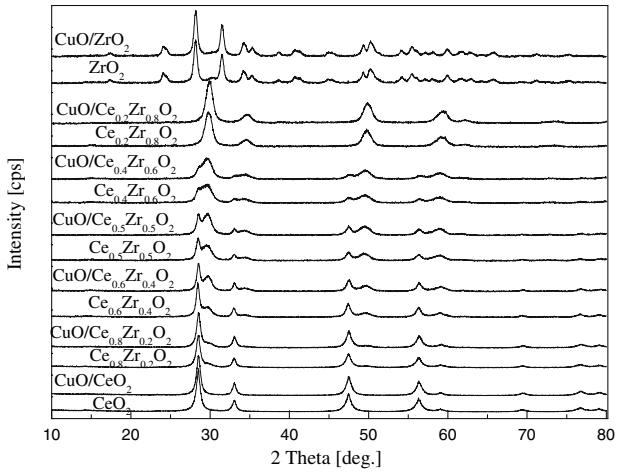

Fig. 1 X-ray diffraction patterns of the supports $Ce_xZr_{1-x}O_2$ and $CuO/Ce_xZr_{1-x}O_2$ catalysts

phase segregation into cerium-rich (cubic fluorite structure) and zirconium-rich (t-ZrO_2) phases. The principal features of $Ce_{0.2}Zr_{0.8}O_2$ support can be ascribed to t-ZrO_2 as seen from the peak at about 30.0° in its XRD pattern. The pure zirconia pattern evidenced that it was monoclinic phase.

In order to discuss the structure of the $Ce_xZr_{1-x}O_2$ samples further, Raman spectroscopy was also carried out. The FT-Raman spectra of the $Ce_xZr_{1-x}O_2$ samples are shown in Fig. 2. The spectrum of $Ce_{0.8}Zr_{0.2}O_2$ showed a similar pattern to pure CeO_2 which only exhibited one peak at 463 cm^{-1}. This is agreement with our previous study [13]. When the Ce content decreased from 0.6 to 0.4, the patterns of the samples exhibited one principal peak at 463 cm^{-1} attributed to cubic fluorite structure and two small peaks at 614, 316 cm^{-1} attributed to the phase of t-ZrO_2. The Raman spectrum of $Ce_{0.2}Zr_{0.8}O_2$ exhibited several peaks at 142, 254, 315, 463 and 626 cm^{-1}. The peak at 463 cm^{-1} is characteristic of cubic fluorite structure, while the peaks at 142, 254, 315 and 626 cm^{-1} can be assigned to the tetragonal phase of ZrO_2 [20]. The FT-Raman spectrum of ZrO_2 showed several major bands at 630, 559, 476, 382, 331, 191 and 177 cm^{-1}, which were mainly assigned to the Raman-active modes for the monoclinic phase of ZrO_2. This is in good agreement with the XRD analyses.

The H_2-TPR profiles of the $CuO/Ce_xZr_{1-x}O_2$ catalysts are presented in Fig. 3. Reduction peaks in the range of 170–300 °C were observed for all the samples and they were attributed to the reduction of CuO species. For the CuO/CeO_2, $CuO/Ce_{0.8}Zr_{0.2}O_2$ and $CuO/Ce_{0.5}Zr_{0.5}O_2$ catalysts, an additional high temperature peak at about 810 °C was present, which was attributed to the reduction of the supports CeO_2, $Ce_{0.8}Zr_{0.2}O_2$ and $Ce_{0.5}Zr_{0.5}O_2$. The peak disappeared when Zr content (1–x) exceeded 0.5.

Several groups have reported the reducibility of CuO supported on Ce–Zr mixed oxides by TPR analyses. Ma et al. [21] reported that the $CuO/Ce_xZr_{1-x}O_2$ catalysts had three reduction peaks, which were attributed to the dispersed copper oxide, the moderate size bulk CuO and the large size bulk CuO, respectively. The catalytic activity was mainly related to the moderate size bulk CuO. Ratnasamy et al. [22] reported that the high dispersion and facile reducibility of CuO on CeO_2 and CeO_2-ZrO_2 supports were responsible for their superior activity. Jiang et al. [23] concluded that the oxidation activity depended on the temperature and shape of the reduction peak of CuO species. In TPR profiles of our samples, two main reduction peaks α and β were observed at about 179 and 201 °C except CuO/ZrO_2. This range of temperature corresponds to the reduction of surface dispersed CuO species [22]. When the fraction (1–x) of incorporated Zr increased to 0.5, a peak γ at about 245 °C appeared and the intensity of

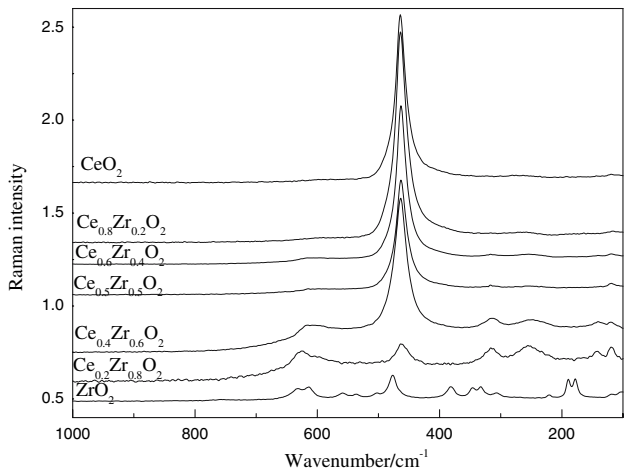

Fig. 2 Raman spectra of the supports $Ce_xZr_{1-x}O_2$

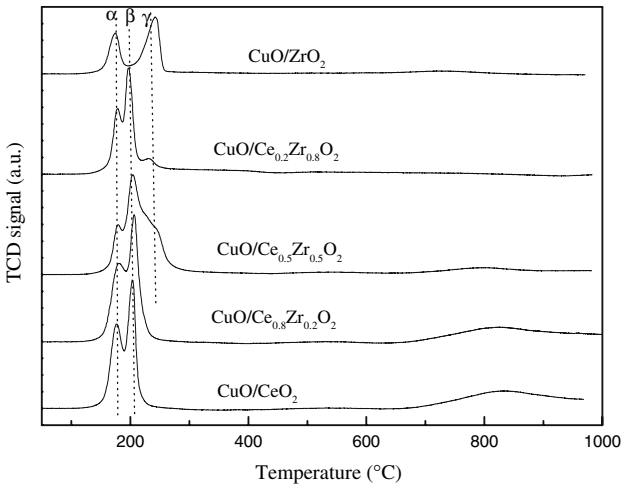

Fig. 3 H_2-TPR profiles of $CuO/Ce_xZr_{1-x}O_2$ catalysts calcined at 500°C 4 h

the peak gradually increased as Zr content increased from 0.5 to 1.0. For CuO/ZrO_2 catalyst, there were also two peaks α and γ presented in the spectrum. According to above analyses, we believed that peak α was attributed to the reduction of highly dispersed CuO which strongly interacts with the support and peak β was attributed to the reduction of larger size CuO which weakly interacts with the support, while peak γ was probably caused by the reduction of bulk CuO. The quantitative analyses for the three peaks α, β and γ were carried out. The result is presented in Table 1 (multi-peaks fitted according to the Gausses method). The CuO/CeO_2 and $CuO/Ce_{0.8}Zr_{0.2}O_2$ catalysts showed better CuO dispersion capacity. As Zr content increased from 0.2 to 1.0, the dispersion capacity of CuO gradually decreased as a function of Ce/Zr ratio. The TPR quantitative results suggested that the dispersion capacity of copper oxide was higher on CeO_2 and $Ce_{0.8}Zr_{0.2}O_2$ than on other supports in this study and it decreased with the increase of Zr content. Furthermore, the reduction temperature of CuO supported on CeO_2 was a little lower than that of CuO supported on $Ce_{0.8}Zr_{0.2}O_2$. Luo et al. [24] have reported that dispersed CuO was responsible for the high catalytic activity of low-temperature CO oxidation. This may make the CuO/CeO_2 and $CuO/Ce_{0.8}Zr_{0.2}O_2$ catalysts show better catalytic property among the $CuO/Ce_xZr_{1-x}O_2$ catalysts and the CuO/CeO_2 catalyst has the highest catalytic activity under the same reaction condition.

Table 1 The quantitative TPR analyses of the $CuO/Ce_xZr_{1-x}O_2$ catalysts

$CuO/Ce_xZr_{1-x}O_2$ (x-value)	H_2 consumption	
	Dispersed copper (α + β) (area percent)	Bulk copper γ (area percent)
1	100	0
0.8	100	0
0.5	83	17
0.2	59	41
0	38	62

X-ray photoelectron spectra is a powerful technique for surface compositional analysis of nano-materials. Figure 4 reveals the presence of cerium, zirconium, copper and oxygen on the surface of CuO(5 wt.%)/$Ce_{0.8}Zr_{0.2}O_2$ catalyst. The Ce 3d XPS BE of the catalyst (Fig. 4a) showed six peaks at about 881.9, 888.6, 898.1, 900.6, 907.3 and 916.1 eV, which was consistent with that of Ce^{4+} species, indicating that the main valence of cerium in CuO(5 wt.%)/$Ce_{0.8}Zr_{0.2}O_2$ was +4. The overlapping peaks at about 181.8 and 184.4 eV showed in Fig. 4b corresponded to the spectra of Zr $3d_{5/2}$ and Zr $3d_{3/2}$, respectively. The peaks of Cu $2p_{3/2}$ and Cu $2p_{1/2}$ were centered at 932.1 and 952.1 eV (Fig. 4c). The binding energy of Cu $2p_{3/2}$ was lower than that of CuO, i.e., 933.6 eV, which suggested the presence of reduced copper species in the catalyst. The XP spectrum of O 1s obtained from the CuO(5 wt.%)/$Ce_{0.8}Zr_{0.2}O_2$ catalyst is shown in Fig. 4d. The binding energy of O 1s was approximately 529.4 eV, which was assigned to the lattice oxygen associated with metal oxides. A broad shoulder at higher B.E. region may be attributed to the oxygen in hydroxyl groups.

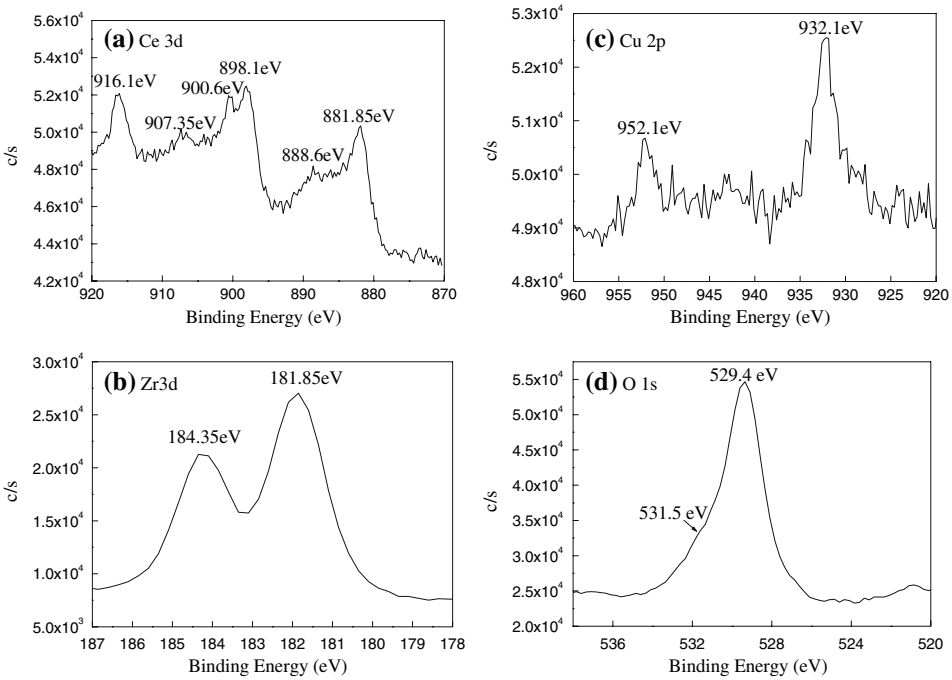

Fig. 4 X-ray photoelectron spectra patterns of CuO/$Ce_{0.8}Zr_{0.2}O_2$ catalysts calcined at 500°C 4 h

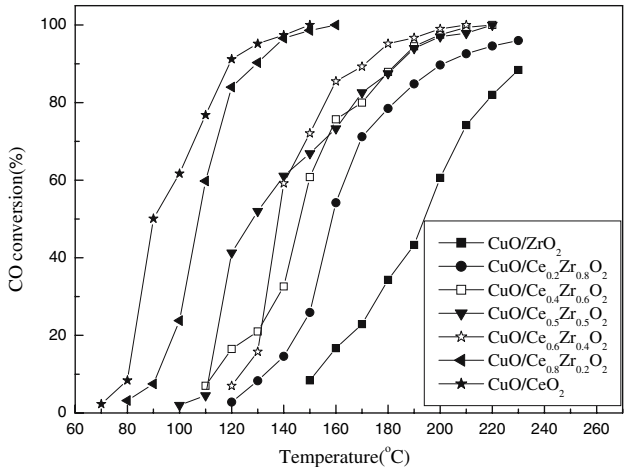

Fig. 5 Catalytic activity for CO oxidation of $CuO/Ce_xZr_{1-x}O_2$ catalysts calcined at 500 °C 4 h

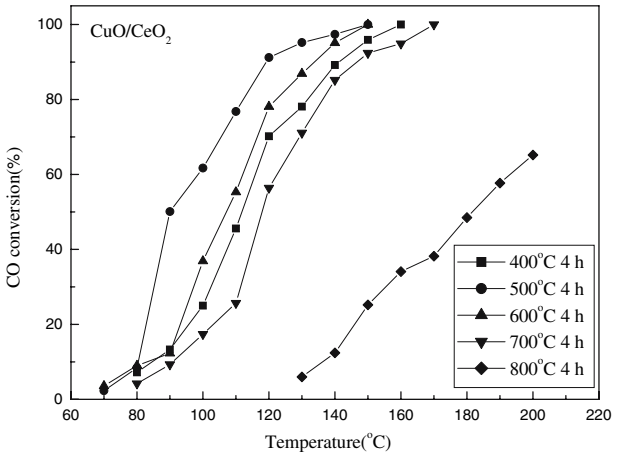

Fig. 6 Catalytic activity for CO oxidation of CuO/CeO_2 catalysts calcined at different temperature

The comparison of the CO oxidation catalytic activities of CuO(5 wt.%)/$Ce_xZr_{1-x}O_2$ catalysts calcined at 500 °C 4 h is shown in Fig. 5. It can be observed that CO conversion increased with the increase of reaction temperature for all the prepared catalysts. The activities of the supports $Ce_xZr_{1-x}O_2$ were similar and quite low (about 20%). Pure ZrO_2 and CuO had no catalytic activity under present condition, however, $Ce_xZr_{1-x}O_2$-supported CuO catalysts showed much higher catalytic activity. The enhancement of the catalytic activity of the catalysts should be attributed to a synergistic effect between CuO and the supports. The "light-off" temperatures (T_{100}) for 100% CO conversion over the CuO(5 wt.%)/$Ce_xZr_{1-x}O_2$ catalysts with Ce fraction x of 1.0, 0.8, 0.6, 0.5 and 0.4 were 150, 160, 210, 220 and 220 °C, respectively. The maximal CO conversion on the CuO(5 wt.%)/$Ce_{0.2}Zr_{0.8}O_2$ and CuO(5 wt.%)/ZrO_2 catalysts were only 96 and 88.4% in this work. We can find that the CO oxidation activity decreased as the content of Ce decreased. Luo et al. [24] suggested that dispersed CuO was responsible for the high CO oxidation catalytic activity. In our previous study, it was concluded that the bulk CuO may deteriorate the catalytic activity [19]. According to the TPR analyses, the CuO/CeO_2 and $CuO/Ce_{0.8}Zr_{0.2}O_2$ catalysts had higher CuO dispersion degree and the dispersion degree of CuO decreased with the increase of Zr content. This may be the reason for the difference of the catalytic activity of the catalysts with different Zr content. The result showed that the CuO/CeO_2 catalyst exhibited the highest catalytic activity and the "light-off" temperature of CuO/CeO_2 catalyst was about 10 °C lower than that of the $CuO/Ce_{0.8}Zr_{0.2}O_2$ catalyst. Furthermore, Compared to $CuO/Ce_{0.8}Zr_{0.2}O_2$ catalyst prepared via other methods by us [13, 19], the catalyst prepared by hydrothermal synthesis combined with impregnation method exhibited better catalytic property. This is probably because that the urea hydrolysis is a mild process to release bases, which make metal ions precipitate homogeneously under controlled pH values [18]. For comparison, the CuO/CeO_2 and $CuO/Ce_{0.8}Zr_{0.2}O_2$ catalysts were further investigated.

The catalytic activities for CO oxidation of CuO/CeO_2 and $CuO/Ce_{0.8}Zr_{0.2}O_2$ catalysts calcined at different temperatures are presented in Figs. 6 and 7, respectively. From Fig. 6, it can be seen that the catalytic activity of the CuO/CeO_2 catalyst increased with the increase of calcination temperature from 400 to 500 °C and the same T_{100} remained when calcined at 500 and 600 °C. However, when the catalyst was calcined above 600 °C the catalytic activity decreased, which may be due to the sinter of the catalyst and the formation of bulk CuO at higher temperature. The T_{100} of the CuO/CeO_2 catalysts calcined at 400, 500, 600 and 700 °C were about 160, 150, 150 and 170 °C, respectively. But the CO conversion of the CuO/CeO_2 catalyst calcined at 800 °C was only about 65% when the reaction temperature reached 200 °C. From Fig. 7, we can see that the $CuO/Ce_{0.8}Zr_{0.2}O_2$ catalysts calcined at 400, 500, 600 °C exhibited similar catalytic behavior, reaching 100% CO conversion at 160 °C. When the calcination temperature exceeded 600 °C, the T_{100} of the CuO/$Ce_{0.8}Zr_{0.2}O_2$ catalysts also raised. The T_{100} of the CuO/$Ce_{0.8}Zr_{0.2}O_2$ catalysts calcined at 700, 800 °C were 180, 190°C, respectively. Compared with the $CuO/Ce_{0.8}Zr_{0.2}O_2$ catalysts, the CuO/CeO_2 catalyst exhibited higher catalytic activity when the calcination temperature was lower than 800 °C. But when they were calcined at 800 °C, the result was just the opposite. This may indicate that incorporating zirconium into CeO_2 can improve the thermal resistance of the resulting mixed oxide, which makes the CuO/$Ce_{0.8}Zr_{0.2}O_2$ catalyst have better thermal resistance than CuO/CeO_2 catalyst. The similar result was also reported in our previous work [13].

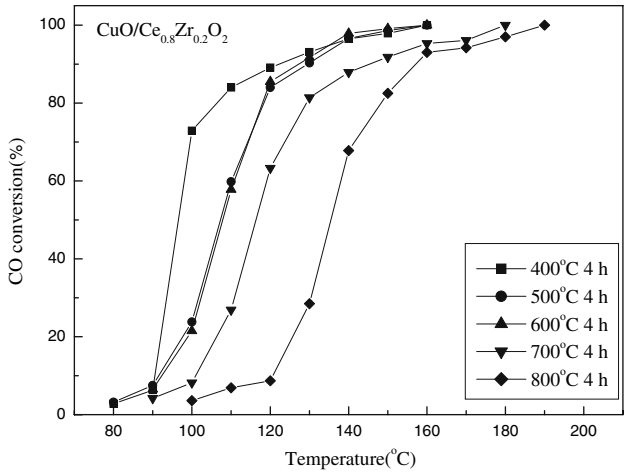

Fig. 7 Catalytic activity for CO oxidation of $CuO/Ce_{0.8}Zr_{0.2}O_2$ catalysts calcined at different temperature

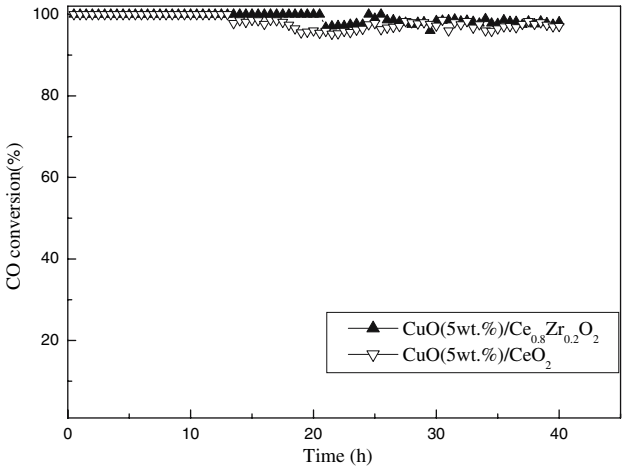

Fig. 8 Deactivation test over CuO/CeO_2 and $CuO/Ce_{0.8}Zr_{0.2}O_2$ catalysts

By catalytic activity tests, it was noted that the catalytic activities of the catalysts for CO oxidation decreased with increasing Zr content, which may be due to the decrease of the CuO dispersion degree on the surface of the supports. This can be identified by the TPR analyses. However, incorporating zirconium into CeO_2 can improve the thermal resistance of the resulting mixed oxide, which makes the $CuO/Ce_{0.8}Zr_{0.2}O_2$ catalyst have better thermal resistance than CuO/CeO_2 catalyst at higher temperature. It can be concluded from the results of catalytic activity tests that the CuO/CeO_2 catalyst showed better catalytic activity than the $CuO/Ce_{0.8}Zr_{0.2}O_2$ catalyst at lower temperature, but the catalytic activity of CuO/CeO_2 catalyst decreased more rapidly than that of $CuO/Ce_{0.8}Zr_{0.2}O_2$ catalyst when the calcination temperature increased to 800 °C.

The lifetime tests of the CuO/CeO_2 and $CuO/Ce_{0.8}Zr_{0.2}O_2$ catalysts were carried out. The results are shown in Fig. 8, which depicts the variation of the catalytic activity for CO oxidation as a function of the reaction time. The catalysts displayed similar trend in deactivation up to 40 h and their CO conversion data changed very slightly during the period. The CuO/CeO_2 catalyst can keep 100% CO conversion for about 13 h, while the $CuO/Ce_{0.8}Zr_{0.2}O_2$ catalyst can keep it for 20.5 h. The result indicated that the addition of Zr into the support can improve the lifetime of the catalyst under given reaction conditions. The investigation also demonstrated that both CuO/CeO_2 and $CuO/Ce_{0.8}Zr_{0.2}O_2$ catalysts were stable.

4 Conclusion

$Ce_xZr_{1-x}O_2$ samples with different Ce/Zr ratios were prepared via a hydrothermal route and used as the supports for $CuO/Ce_xZr_{1-x}O_2$ catalysts. The influence of the Ce/Zr ratios on the structure and catalytic activity of $CuO/Ce_xZr_{1-x}O_2$ catalysts was investigated. From TPR analyses, it can be concluded that the CuO dispersion degree on the surface of supports decreased with the increase of Zr content. The XPS analysis indicated that the valence of Ce atom in the prepared $CuO/Ce_{0.8}Zr_{0.2}O_2$ catalyst was +4 and there were reduced copper species dispersed on the catalyst surface. In the CO oxidation reaction, the catalytic activity decreased as the content of Ce decreased and the CuO/CeO_2 catalyst exhibited the highest catalytic activity. However, incorporation of zirconium into CeO_2 can improve the thermal resistance of the catalyst. The $CuO/Ce_{0.8}Zr_{0.2}O_2$ catalyst had better catalytic property than CuO/CeO_2 catalyst when they were both calcined at 800 °C. The results of TPR analyses and catalytic activity tests indicated that the Ce/Zr ratio had effect on the CuO dispersion degree of the $CuO/Ce_xZr_{1-x}O_2$ catalysts and the dispersed CuO was responsible for the high catalytic activity of CO oxidation. Both CuO/CeO_2 and $CuO/Ce_{0.8}Zr_{0.2}O_2$ catalysts exhibited stable activity for 40 h experiments.

Acknowledgment This work was supported by the National Natural Science Foundation of China (No. 20771061).

References

1. Min K, Song MW, Lee CH (2003) Appl Catal A 251:143
2. Pillai UR, Deevi S (2006) Appl Catal B 65:110
3. Wang Y-Q, Caruso RA (2002) J Mater Chem 12:1442
4. Bechara R, Wrobel G, Aissi CF, Guelton M, Bonnelle JP, Abou-Kais A (1990) Chem Mater 2:518
5. Huang J, Wang S-R, Zhao Y-Q, Wang X-Y, Wang S-P, Wu S-H, Zhang S-M, Huang W-P (2006) Catal Commun 7:1029
6. Cheng T, Fang Z-Y, Hu Q-X, Han K-D, Yang X-Z, Zhang Y-J (2007) Catal Commun 8:1167

7. Jiang X-Y, Zhou R-X, Pan P, Zhu B, Yuan X-X, Zheng X-M (1997) Appl Catal A 150:131
8. Luo M-F, Ma J-M, Lu J-Q, Song Y-P, Wang Y-J (2007) J Catal 246:52
9. Zheng X-C, Wu S-H, Wang S-P, Wang S-R, Zhang S-M, Huang W-P (2005) Appl Catal A 283:217
10. Monte RD, Kašpar J (2005) Catal Today 100:27
11. Liu X-Y, Wang S-D, Yuan Z-S, Zhou J, Liu N, Zhang C-X, Fu G-Z (2004) Chin J Catal 2:91
12. Kakuta N, Ikawa S, Eguchi T, Murakami K, Ohkita H, Mizushima T (2006) J Alloys Compd 1078:408–412
13. Wang S-P, Zheng X-C, Wang X-Y, Wang S-R, Zhang S-M, Yu L-H, Huang W-P, Wu S-H (2005) Catal Lett 105:163
14. Terribile D, Trovarelli A, Llorca J, Leitenburg CD, Dolcetti G (1998) Catal Today 43:79
15. Otsuka K, Wang Y, Nakamura M (1999) Appl Catal A 183:317
16. Trovarelli A, Zamar F, Llorca J, deLeitenburg C, Dolcetti G, Kiss JT (1997) J Catal 169(2):490–502
17. Liotta LF, Macaluso A, Longo A, Pantaleo G, Martorana A, Deganello G (2003) Appl Catal A 240:295
18. Si R, Zhang Y-W, Xiao C-X, Li S-J, Lin B-X, Kou Y, Yan C-H (2004) Phys Chem Chem Phys 6:1056
19. Wang S-P, Wang X-Y, Huang J, Zhang S-M, Wang S-R, Wu S-H (2007) Catal Commun 8:231
20. Pokrovski KA, Bell AT (2006) J Catal 241:276
21. Ma L, Luo M-F, Chen S-Y (2003) Appl Catal A 242:151
22. Ratnasamy P, Srinivas D, Satyanarayana CVV, Manikandan P, Kumaran RSS, Sachin M, Shetti VN (2004) J 'Catal 221:455
23. Jiang X-Y, Zhou R-X, Chen Y, Lou L-P, Zheng X-M (2001) J Zhejiang Univ (Science Edition) 28(6):653
24. Luo M-F, Hou Y-Y, Yuan X-X, Zheng X-M (1998) Catal Lett 50:205